Landau Level Spectroscopy of Ultrathin Graphite Layers

M. L. Sadowski, G. Martinez, and M. Potemski
Grenoble High Magnetic Field Laboratory, CNRS, Grenoble, France

C. Berger* and W. A. de Heer
Georgia Institute of Technology, Atlanta, Georgia, USA
(Received 30 May 2006; published 28 December 2006)

Far infrared transmission experiments are performed on ultrathin epitaxial graphite samples in a magnetic field. The observed cyclotron resonancelike and electron-positron-like transitions are in excellent agreement with the expectations of a single-particle model of Dirac fermions in graphene, with an effective velocity of $\tilde{c} = 1.03 \times 10^6$ m/s.

DOI: 10.1103/PhysRevLett.97.266405 PACS numbers: 71.70.Di, 76.40.+b, 78.30.−j, 78.67.−n

The electronic properties of graphite have recently become the center of considerable attention, following experiments on graphite monolayers (graphene) [1] and epitaxial praphene [2], which led to the discovery of an unusual sequence of quantum Hall effect states [3,4] and an energy-dependent mass. The considerable interest in two-dimensional graphite is fueled by its particular band structure and ensuing dispersion relation for electrons, leading to numerous differences with respect to ''conventional'' two-dimensional electron systems (2DES) [2,5–12]. The band structure of graphene is considered to be composed of cones located at two inequivalent Brillouin zone corners at which the conduction and valence bands merge. In the vicinity of these points the electron energy depends linearly on its momentum: $E(\vec{p}) = \pm\tilde{c}|\vec{p}|$, which implies that free charge carriers in graphene are governed not by Schrödinger's equation, but rather by Dirac's equation for zero rest mass particles, with an effective velocity $\tilde{c}$, which replaces the speed of light. With the application of an external magnetic field, the Dirac energy spectrum evolves into Landau levels with energies given by

$$E_n = \mathrm{sgn}(n)\tilde{c}\sqrt{2e\hbar B|n|} = \mathrm{sgn}(n)E_1\sqrt{|n|}, \qquad (1)$$

where n scans all positive (for electrons) and negative (for holes) integers and, very importantly, zero. E_1 may be understood as a characteristic energy introduced by the magnetic field. The square root dependence on B and Landau level index n is in stark contrast to conventional 2D electrons, where $E_n = (n + \frac{1}{2})\hbar eB/m$, $(n \geq 0)$, and the Landau levels are equally spaced.

The unusual sequence of quantum Hall effect states and an energy-dependent electron effective mass [3,4], found in magnetoresistance measurements, are consistent with the model of Dirac particles. Here we report a magneto-spectroscopy study of the optical properties of ultrathin epitaxial graphite layers, in which we directly probe the dependence of the energy of electrons on their momentum.

The experiments were performed on graphene layers grown in vacuum by the thermal decomposition method [2,12], on single crystal (4H) SiC. These epitaxial graphene structures are routinely characterized using low energy electron diffraction, Auger electron spectroscopy, x-ray diffraction, scanning tunneling microscopy and atomic force microscopy. The results of these measurements in combination with angular resolved photoelectron spectroscopy and transport data indicate that the graphitized part of this type of structure consists of a few (3–5) graphene layers [2,12]. We investigated two such (unpatterned) structures, with dimensions of about 4×4 mm^2, which both show a similar behavior.

The far infrared transmission of the samples was measured, at a temperature of 1.9 K, as a function of the magnetic field B. A Si bolometer was placed directly beneath the sample to detect the transmitted radiation. The light (provided and analyzed by a Fourier transform spectrometer) was delivered to the sample by means of light-pipe optics. All experiments were performed with nonpolarized light, in the Faraday geometry with the wave vector of the incoming light parallel to the magnetic field direction. The transmission spectra were normalized by the transmission of the substrate and by the zero-field transmission, thus correcting for magnetic field induced variations in the response of the bolometer. The SiC substrate used was completely opaque for energies between 85 meV and about 200 meV, which limited the range of our investigation.

The main experimental finding consists of several absorption lines visible in the spectra. A representative transmission spectrum for sample 1, at 0.4 T, is shown in Fig. 1. These lines evolve spectacularly with the magnetic field. Two main lines are shown in Fig. 2 for several values of the field. As shown in Fig. 3, their energies, plotted as a function of the square root of the magnetic field, trace perfect straight lines, in excellent agreement with Eq. (1). Also shown in this figure are the energy positions of the two other lines. Experiments performed in a tilted configuration show that the position of the transition line (solid symbols in Fig. 3) depends only on the component of the magnetic field perpendicular to the sample plane. A complicated structure at still lower energies, not shown in the

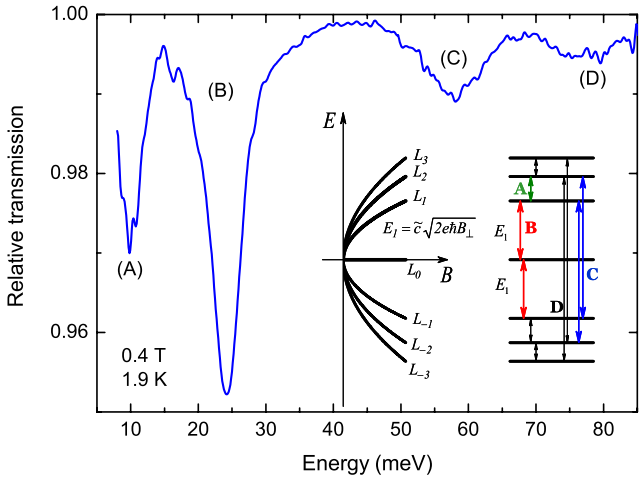

FIG. 1 (color online). Relative transmission trace at 0.4 T and 1.9 K shows four distinct transitions. The assignations are (see text) A: $L_1 \rightarrow L_2$, B: $L_0 \rightarrow L_1(L_{-1} \rightarrow L_0)$, C: $L_{-2} \rightarrow L_1(L_{-1} \rightarrow L_2)$, D: $L_{-3} \rightarrow L_2(L_{-2} \rightarrow L_3)$. The inset shows a schematic of the evolution of Landau levels with applied magnetic field, and possible optical transitions.

figure, moving slowly to higher energies with magnetic field, was also observed. Unusually, the intensities of the two main lines increase markedly with increasing magnetic field, with the lower-energy line always remaining stronger.

Cyclotron resonance in graphite has been studied experimentally [13] and theoretically [14,15]. These experiments showed a linear dependence of the cyclotron frequency on the magnetic field, with an effective mass of $0.058m_0$. Our results are best described using the predictions of a simple single-particle (Dirac) model for a graphene layer, and we will use this language in the following paragraphs. To facilitate discussion, we sketch the graphene Landau levels and possible transitions between them in the inset to Fig. 1.

Thus, we assign the strongest line to the transitions to and from the lowest Landau level. Note that, since the conduction and valence band states in graphene are built from the same atomic orbitals, the positive and negative branches of the dispersion relation are identical. The ensuing symmetry means that the $L_0 \rightarrow L_1$ and $L_{-1} \rightarrow L_0$ transitions are indistinguishable in an experiment using unpolarized radiation. A straight line fit of the points corresponding to this transition using the expression $E = E_1 = \tilde{c}\sqrt{2e\hbar B}$ yields a very accurate value for $\tilde{c}$, the velocity of electrons in graphene. This is found for both samples to be $(1.03 \pm 0.01) \times 10^6$ m/s, consistently with transport measurements [3,4].

The slopes of the other lines traced in Fig. 3, starting from the highest energy transition, scale exactly as $(\sqrt{3} + \sqrt{2}):(\sqrt{2} + 1):1:(\sqrt{2} - 1)$, allowing these lines to be assigned to transitions $L_{-2} \rightarrow L_3(L_{-3} \rightarrow L_2)$, $L_{-1} \rightarrow L_2(L_{-2} \rightarrow L_1)$, $L_0 \rightarrow L_1(L_{-1} \rightarrow L_0)$, and $L_1 \rightarrow L_2$, respectively, as shown in the figure.

The fact that transitions involving the L_0 Landau level are visible at such low magnetic fields places an upper limit on the electron concentration in the observed layer. The

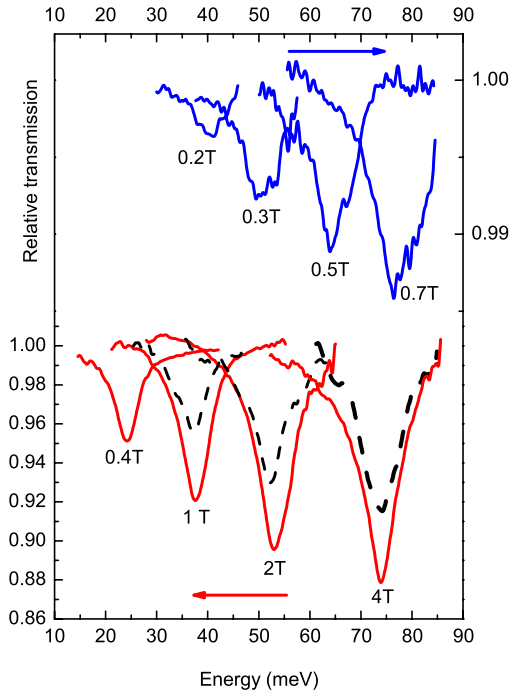

FIG. 2 (color online). Development of two main transmission lines with the magnetic field. Upper panel shows the line marked C in Fig. 1, corresponding to $L_{-1} \rightarrow L_2(L_{-2} \rightarrow L_1)$ transitions; lower panel shows the line marked B, corresponding to $L_0 \rightarrow L_1(L_{-1} \rightarrow L_0)$ transitions: solid lines are for sample 1, dashed lines for sample 2.

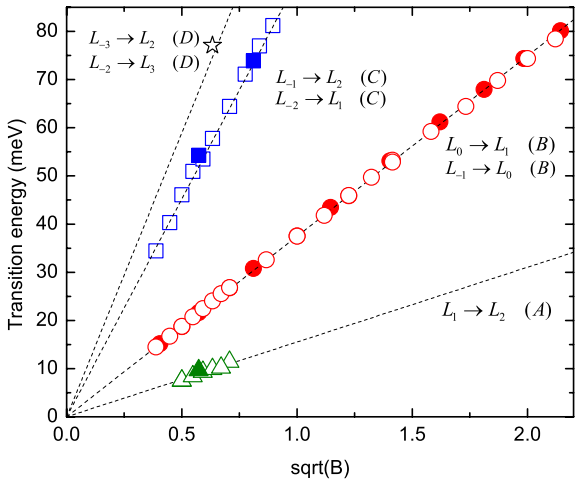

FIG. 3 (color online). The observed transitions, together with their assignments, plotted versus $B_\perp$. The solid symbols are data obtained for the sample tilted with respect to the direction of B by an angle of 50°. The dashed lines are all calculated with the same characteristic velocity $\tilde{c} = 1.03 \times 10^6$ m/s.

observation of the $L_0 \rightarrow L_1 (L_{-1} \rightarrow L_0)$ line implies the existence of unpopulated states at least on the L_1 level. This line is clearly observed at fields $B \approx 0.15$ T, and therefore the L_1 level can be fully populated only when $B < 0.15$ T. Thus $n \leq 2.1 \times 10^{10}$ cm^{-2} (where we take into account the twofold and fourfold degeneracy of the L_0 and L_1 electronic Landau levels, respectively). This is also consistent with the disappearance of line A $(L_1 \rightarrow L_2)$ when the L_1 level is depopulated by the magnetic field (see Fig. 3).

We now turn our attention to the strength of the transitions. As may be seen in Fig. 2, both the main transitions gain in intensity with increasing magnetic field. To better visualize this trend, we plot the integrated intensity (area under the dip in the relative transmission) for sample 1, as a function of the square root of the magnetic field (Fig. 4). Sample 2 shows the same behavior but smaller values of the intensity.

The relative transmission of a sheet of conducting electrons between vacuum and a dispersionless polar medium with a refractive index κ, for unpolarized radiation and in the limit of weak absorption, may be written as (see, e.g., [16,17])

$$T(\omega, B) \approx 1 - \beta \frac{\mathrm{Re}[\sigma_{xx}(\omega, B)]}{\epsilon_0 c},$$

where $\sigma_{xx}(\omega, B)$ is a diagonal element of the optical conductivity tensor, ϵ_0 is the vacuum permittivity, c is the speed of light in vacuum, and $\beta = (\kappa^2 + 3)/2(\kappa^2 + 1) = 0.63$ for SiC, where $\kappa = 2.6$ (from the substrate transmission). The optical conductivity of the 2D electrons may be written using the Kubo formalism [18] and taking into account the properties of the graphene Landau level wave functions [8,19]

$$\sigma_{xx}(\omega, B) = \frac{4 G_B e^2}{\omega} \sum_{m,n} \frac{(f_m - f_n) M_{m,n}}{E_{m,n} - (\hbar\omega + i\gamma)},$$

where $E_{m,n}$ are the transition energies between levels m and n, $G_B = eB/h$ is the Landau level degeneracy, f_m, f_n are the occupancies of the relevant Landau levels and the selection rules for the optically active transitions are given by $M_{m,n} = (\tilde{c}^2/p)\delta_{|m|,|n|\pm 1}$, with $p = 2$ for m or $n = 0$ and 4 otherwise. The summation is performed over all Landau levels m, n, and the fourfold degeneracy of each Landau level has already been accounted for.

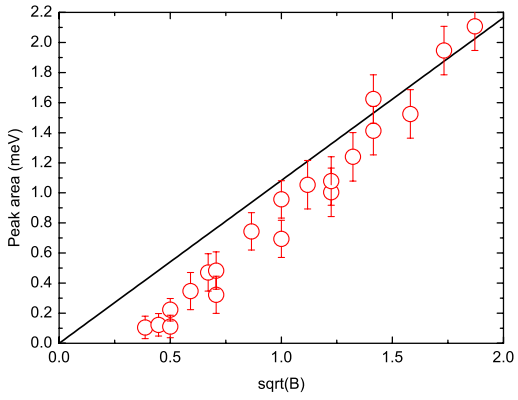

FIG. 4 (color online). Area of the main peak observed in the experiments, the $L_0 \rightarrow L_1 (L_{-1} \rightarrow L_0)$ transition, plotted against the square root of the magnetic field. The line is traced using the expression $\beta(e^2/2\epsilon_0\hbar c)E_1$.

The integrated transmission for a single transition between a completely solid (L_0) and a completely empty (L_1) Landau level, using the above expression (for linewidths $\gamma \ll E_{m,n}$) may be written as

$$I(B) = \frac{1}{\epsilon_0 c} \int \mathrm{Re}(\sigma_{xx}(\omega)) d\omega \approx \frac{e^3 \tilde{c}^2 B}{\epsilon_0 c E_1} = \beta \frac{e^2 \tilde{c}}{2\epsilon_0 \hbar c} E_1,$$

where E_1 is the characteristic energy introduced earlier.

The above equation gives a rough estimate of the intensity of the strongest transition, in the range of high magnetic fields where the Fermi energy is pinned to the L_0 level. This is due to the fact that the decreasing intensity of the $L_0 \rightarrow L_1$ transition is compensated by the corresponding increase of the strength of the superimposed $L_{-1} \rightarrow L_0$ transition. At low magnetic fields, where the L_1 level is not completely empty, the observed oscillator strength decreases, disappearing when the L_1 is fully populated. In spite of the rather crude approximation, Fig. 4 indeed shows that the observed transition follows the expected trend; the good agreement of the absolute measured and calculated values is another factor supporting the picture of a single, possibly inhomogeneous, graphene layer (see discussion in following paragraphs).

Several notable differences emerge between Dirac electrons and conventional two-dimensional electron systems (2DES). As we have shown, transitions between adjacent Landau levels in graphene occur at markedly different energies (for example $L_0 \rightarrow L_1$ and $L_1 \rightarrow L_2$, Figs. 1 and 3). For a standard 2DES, transitions between such pairs of Landau levels all have the same energy. More striking, a different class of transitions, with no counterpart in a standard 2DES, is observed in graphene and involves those from hole $(n < 0)$ to electron $(n > 0)$ states (e.g., our $L_{-1} \rightarrow L_2$ and $L_{-2} \rightarrow L_1$ transitions). These are the particle-antiparticle creation and annihilation events in the Dirac formalism.

Since some of the observed transitions are analogues of cyclotron resonance, it is tempting to look at them in a semiclassical context, using the concept of an effective mass. While for a 2DES with a quadratic dispersion law there is a coincidence between classical and quantum mechanical solutions of the optically active response in a magnetic field, this does not hold for graphene. The classically derived cyclotron excitation E_C in this system is $E_C = \hbar eB/(E/\tilde{c}^2)$ [8], where E is the electron energy and $(E/\tilde{c}^2)$ stands for the electron mass. Although the effective rest mass of the electrons in graphene is zero, their energy- and magnetic field-dependent cyclotron mass can be fol-

lowed down to the lowest energies (≃7 meV in our case), giving a lowest observed value of $0.0012m_0$.

Having demonstrated the presence of zero effective rest mass Dirac fermions in the investigated structure, let us now consider the following points: (i) linear dispersion is characteristic of a single graphene layer, while a graphene bilayer [20,21] is found to exhibit parabolic dispersion; (ii) transport measurements performed on a mesoscopic sample patterned on the same wafer as our selected sample, which also show the unusual Berry's phase of π observed in graphene, give a concentration of $\simeq 4 \times 10^{12}$ cm^{-2}, while our results point to a concentration 2 orders of magnitude smaller.

It is believed that electric transport is dominated by the interface layer, which has a high-electron concentration due to the built-in electric field caused by the surface charge [2,22]. Transmission measurements, on the other hand, probe the whole sequence of layers, including those further away from the interface which have lower electron concentrations. It is possible that the observed Dirac spectrum originates from a single graphene layer "floating" above a SiC substrate covered with other graphitic layers [23]. The previously mentioned very low-energy features in our spectra could arise from the high-electron-concentration parts of the sample, where the energy difference between adjacent Landau levels is small.

Another factor possibly affecting the data could be lateral inhomogeneity within a single graphene plane, or even fragmentation of the layer; this could explain the weaker intensities observed for sample 2. Individual graphene planes in epitaxial graphite may be much more weakly coupled than is usually accepted for graphite. Several graphene layers [24] may, depending on the stacking scheme, exhibit linear and/or parabolic dispersion relations. Finally, we note that carriers with linear dispersion may also be found at the H point of bulk graphite [25–27], although the significant difference between the value of $\tilde{c}$ found in [27] (0.91×10^6 m/s) and our experiment, as well as the structure of the samples, makes such an interpretation unlikely. The current experiment shows an absorption in good agreement with that expected for graphene, but the simple approximation used does not exclude more complex scenarios.

Concluding, we have measured the optical excitation spectrum of (relativisticlike) Dirac fermions in a condensed matter system. These fermions are found in thin layers of epitaxial graphite, probably in single (or extremely weakly coupled) graphene layers (or parts of layers). Cyclotron resonancelike transitions coexist with electron-hole (particle-antiparticle)-like transitions, with energy positions and oscillator strengths in surprisingly good agreement with expectations based on a model of noninteracting particles with linear dispersion.

The GHMFL is a "Laboratoire conventionné avec l'UJF et l'INPG de Grenoble." The present work was supported in part by the European Commission through Grant No. RITA-CT-2003-505474 and by grants from the Intel Research Corporation and the NSF: NIRT "Electronic Devices from Nano-Patterned Epitaxial Graphite."

*also at LEPES, CNRS Grenoble, France

[1] K. S. Novoselov, A. K. Geim, S. V. Morozov, D. Jiang, M. I. Katsnelson, I. V. Grigorieva, S. V. Dubonos, and A. A. Firsov, Science **306**, 666 (2004).
[2] C. Berger, Z. Song, T. Li, X. Li, X. Wu, N. Brown, C. Naud, D. Mayou, A. N. Marchenkov, and E. H. Conrad *et al.*, Science **312**, 1191 (2006).
[3] K. S. Novoselov, A. K. Geim, S. V. Morozov, D. Jiang, M. I. Katsnelson, I. V. Grigorieva, S. V. Dubonos, and A. A. Firsov, Nature (London) **438**, 197 (2005).
[4] Y. Zhang, Y.-W. Tan, H. L. Stormer, and P. Kim, Nature (London) **438**, 201 (2005).
[5] P. R. Wallace, Phys. Rev. **71**, 622 (1947).
[6] J. W. McClure, Phys. Rev. **104**, 666 (1956).
[7] F. D. M. Haldane, Phys. Rev. Lett. **61**, 2015 (1988).
[8] Y. Zheng and T. Ando, Phys. Rev. B **65**, 245420 (2002).
[9] V. P. Gusynin and S. G. Sharapov, Phys. Rev. Lett. **95**, 146801 (2005).
[10] V. P. Gusynin, S. G. Sharapov, and J. P. Carbotte, Phys. Rev. Lett. **96**, 256802 (2006).
[11] N. M. R. Peres, F. Guinea, and A. H. Castro Neto, Phys. Rev. B **73**, 125411 (2006).
[12] C. Berger, Z. Song, T. Li, X. Li, A. Y. Ogbazghi, R. Feng, Z. Dai, A. N. Marchenkov, E. H. Conrad, and P. N. First *et al.*, J. Phys. Chem. **108**, 19 912 (2004).
[13] J. K. Galt, W. A. Yager, and J. H. W. Dail, Phys. Rev. **103**, 1586 (1956).
[14] P. Nozières, Phys. Rev. **109**, 1510 (1958).
[15] M. Inoue, J. Phys. Soc. Jpn. **17**, 808 (1962).
[16] K. W. Chiu, T. K. Lee, and J. J. Quinn, Surf. Sci. **58**, 182 (1976).
[17] T. Ando, J. Phys. Soc. Jpn. **38**, 989 (1975).
[18] R. Kubo, J. Phys. Soc. Jpn. **12**, 570 (1957).
[19] T. Ando, Y. Zheng, and H. Suzuura, J. Phys. Soc. Jpn. **71**, 1318 (2002).
[20] E. McCann and V. I. Fal'ko, Phys. Rev. Lett. **96**, 086805 (2006).
[21] K. S. Novoselov, E. McCann, S. V. Morozoz, V. I. Fal'ko, M. I. Katsnelson, U. Zeitler, D. Jiang, F. Schedin, and A. K. Geim, Nature Phys. **2**, 177 (2006).
[22] P. B. Visscher and L. M. Falicov, Phys. Rev. B **3**, 2541 (1971).
[23] I. Forbeaux, J.-M. Themlin, and J.-M. Debever, Phys. Rev. B **58**, 16 396 (1998).
[24] F. Guinea, A. H. Castro Neto, and N. M. R. Peres, Phys. Rev. B **73**, 245426 (2006).
[25] W. W. Toy, M. S. Dresselhaus, and G. Dresselhaus, Phys. Rev. B **15**, 4077 (1977).
[26] B. Partoens and F. M. Peeters, Phys. Rev. B **74**, 075404 (2006).
[27] S. Y. Zhou, G.-H. Gweon, J. Graf, A. V. Fedorovo, C. D. Spataru, R. D. Diehl, Y. Kopelevich, D.-H. Lee, S. G. Louie, and A. Lanzara, Nature Phys. **2**, 595 (2006).